

Article

Heat Treatment at 1000 °C under Reducing Atmosphere of Commercial Vermiculites

Ayoub Lahchich ¹, Pedro Álvarez-Lloret ¹ , Fabrice Leardini ²  and Celia Marcos ^{1,*} 

¹ Department de Geología, Facultad de Geología, Universidad de Oviedo, C/. Jesús Arias de Velasco s/n, 33005 Oviedo, Spain; uo285853@uniovi.es (A.L.); pedroalvarez@uniovi.es (P.Á.-L.)

² Department de Física de Materiales M-04, Facultad de Ciencias, Universidad Autónoma de Madrid, Cantoblanco, 28049 Madrid, Spain; fabrice.lear dini@uam.es

* Correspondence: cmarcos@uniovi.es; Tel.: +34-985103100

Abstract: With the purpose of obtaining synthetic materials from other natural sources for industrial and technological applications, a thermal alteration study was carried out with commercial vermiculites of different purity and origin. For this objective, samples were subjected to 1000 °C in a furnace both at ambient and reduced (N₂/Ar) atmospheres. The thermal behavior and physicochemical properties of the different vermiculites were investigated by X-ray diffraction (XRD), thermal analysis (TG and DTG), and scanning electron microscopy (SEM), and their textural parameters were analyzed by BET treatment. The transformations undergone by the investigated commercial vermiculites subjected to heating treatments caused textural and structural changes in them. There was a decrease in the specific surface area, adsorption capacity, and pore volume values for the samples treated with in situ heating at 1000 °C, both at ambient and reduced atmospheres, and the samples were treated with ex situ abrupt heating at 1000 °C at ambient conditions. There was a decrease in the specific surface area, adsorption capacity, and pore volume values for the samples treated with in situ heating at 1000 °C, both in ambient and reduced atmospheres, which was not observed in the samples treated with an ex situ abrupt heating at 1000 °C at ambient conditions. This corroborated with our findings that the expansion in the first type of thermal treatment produced less separation of the exfoliation sheets than the expansion in the second type of thermal treatment. These textural changes, together with the structural ones, could play a fundamental role in the choice of industrial and technological applications for which these materials could be used.

Keywords: vermiculites; reducing atmosphere; adsorption; heating; polluting substances



Citation: Lahchich, A.; Álvarez-Lloret, P.; Leardini, F.; Marcos, C. Heat Treatment at 1000 °C under Reducing Atmosphere of Commercial Vermiculites. *Minerals* **2024**, *14*, 232. <https://doi.org/10.3390/min14030232>

Academic Editors: Ana María Fernández and Luca Aldega

Received: 30 November 2023

Revised: 20 February 2024

Accepted: 23 February 2024

Published: 25 February 2024



Copyright: © 2024 by the authors. Licensee MDPI, Basel, Switzerland. This article is an open access article distributed under the terms and conditions of the Creative Commons Attribution (CC BY) license (<https://creativecommons.org/licenses/by/4.0/>).

1. Introduction

Vermiculite is a silicate mineral of the phyllosilicate subclass. Its appearance is similar to that of micas at the macroscopic level, and it shows varied colors (green and yellow to brown), leafy habit, a hardness of around 2, and a density between 2.4 and 2.7 g/cm³. Its structure corresponds to that of the 2:1 group [1], which is composed of two T-O-T layers joined by an interlayer. The T-O-T layer is composed of an octahedral (O) sheet of Mg²⁺ located between two tetrahedral sheets (T) of Si⁴⁺. The interlayer contains water molecules and exchangeable cations, mainly Mg²⁺ ions. Isomorphic substitutions, especially in the tetrahedral sheets of Si⁴⁺ to Al³⁺, are very common. Vermiculite can undergo hydration-dehydration processes due to the presence of water and OH⁻ groups that depend on various factors such as temperature, pressure, particle size, relative humidity, and chemical composition [1–17].

The materials of this research are commercial vermiculites of different origins and properties. Vermiculite, a low-cost mineral with abundant reserves, easy exfoliation, high porosity, and specific surface area [18–21], makes it a CO₂ substrate, like amines [22] or calcium oxide [23]. Due to its particular physicochemical properties (mainly related to its thermal resistance and exfoliation capacity), vermiculite offers multiple industrial and

technological applications. Vermiculite is widely employed in the construction industry mainly for its insulating and lightweight characteristics (i.e., concrete production, plasters, renders, fireproof, and thermal screeds) [24,25]. Furthermore, the particle size and intrinsic porosity of vermiculite are also advantageous properties for numerous technological uses, such as chemical process catalysts and fluid filtration supports [26–28]. A recent study has also shown how the structural features of vermiculites give them even further potential applications in biomedical engineering (i.e., cancer theranostics) [29]. Overall, these technological applications highlight the versatility of vermiculite, as its properties can be modified by physical, chemical, or mechanical treatments depending on the requirements of each industry and application.

Vermiculite is characterized by its unique thermal expansion properties and is of considerable usefulness for the technological and industrial applications described above. This mineral property can vary depending on factors such as the specific type of vermiculite (related to its composition) and the temperature and heating condition to which it is exposed.

This study was carried out by heating at 1000 °C three different commercial vermiculites both at ambient and reduced atmospheres in order to obtain other materials with industrial and technological applications. The response of the investigated vermiculites to the mentioned thermal treatment was studied by X-ray diffraction, thermal analysis, and scanning electron microscopy, and their adsorption capacity was analyzing variations in textural parameters (i.e., BET-specific surface area and porosity), using nitrogen adsorption/desorption tests.

2. Materials and Methods

2.1. Materials

The materials investigated in this paper were vermiculites; one vermiculite came from Uganda and was supplied by the company Vermiculita y Derivados S.L. (Gijón, Spain); it was labeled as U. The other vermiculites came from China, and they were supplied by China National Non-Metallic Minerals Industrial Import & Export Corporation (CNMIEC) (Beijing, China); they were labeled as CHS and CHGO, respectively. The particle size of all vermiculites is <5 mm in diameter, and the thickness varies from 0.5 to 1 mm. With respect to their appearance, The Ugandan vermiculite and the Chinese CHGO are golden in color, and the Chinese vermiculite CHS is silver in color (Figure 1).

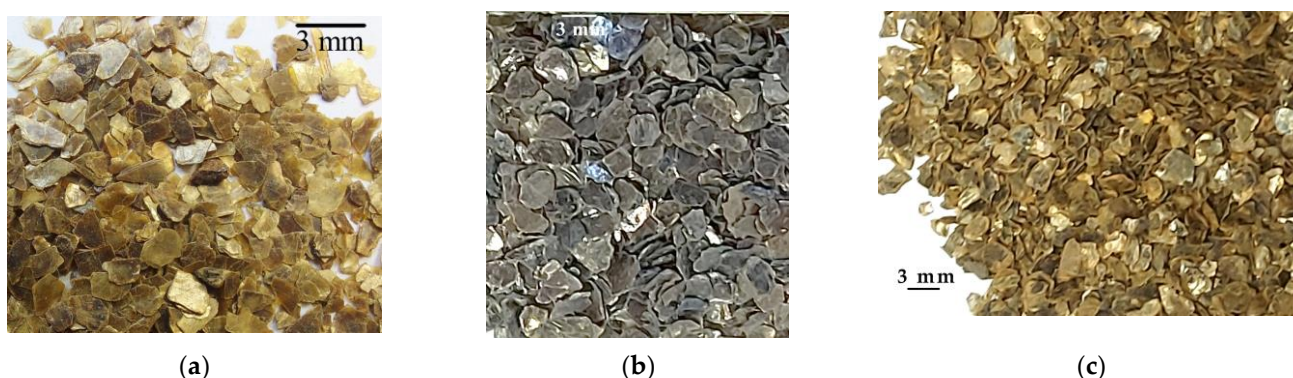


Figure 1. Appearance of the investigated vermiculites in hand sample: (a) U, (b) CHS, (c) CHGO.

2.2. Experiments

Experiments at high temperatures were conducted using the raw vermiculites without previous treatment in order to preserve their natural characteristics as much as possible.

The experiments were carried out using the Carbolite Gero EZS 1200 Ltd. (Sheffield, UK) furnace under ambient atmosphere and reducing atmosphere. Once the samples were placed in the sample holders, the furnace was programmed to 1000 °C at 20 °C/min steps. After reaching the programmed temperature, the samples were kept for 1 h and then cooled.

The experiments with reduced atmosphere were carried out under controlled atmospheres of H₂ and Ar: (a) 100% H₂, (b) 100% Ar, and (c) 5% H₂ and 95% Ar. The gas flow rate was 100 sccm in each experiment. Vermiculites were weighed before and after each heat treatment. These experiments are hereafter referred to as in situ heating at 1000 °C in ambient atmosphere and in situ heating at 1000 °C in reduced atmosphere.

The samples were labeled as shown in Table 1.

Table 1. Labels of the high-temperature heated vermiculite samples.

Ambient	High-Temperature Thermal Treatment		
	100% Ar	5% H ₂ /95% Ar	100% H ₂
U-1000	U-1000-Ar	U-1000-5H ₂ /95Ar	U-1000-H ₂
CHS-1000	CHS-1000-Ar	CHS-1000-5H ₂ /95Ar	CHS-1000-H ₂
CHGO-1000	CHGO-1000-Ar	CHGO-1000-5H ₂ /95Ar	CHGO-1000-H ₂

For the purposes of comparison of certain results to be shown below, high-temperature thermal experiments in the ambient atmosphere were also carried out using the Carbolite CWF 12/23 type furnace. The furnace was first stabilized at a temperature of 1000 °C. Then, the vermiculite samples were introduced and heated for 1 min, after which it was removed and allowed to cool at room temperature. These experiments are hereafter referred to as ex situ abrupt heating at 1000 °C in ambient atmosphere.

2.3. Sample Characterizations

Raw and treated vermiculites were subjected to characterization of the elemental composition using X-ray fluorescence, identification of the mineral composition by X-ray diffraction (XRD), thermal behavior using thermal gravimetric (TG and DTG), and analysis of textural parameters with BET treatment.

The chemical composition of the raw vermiculites was determined using an X-ray fluorescence spectrometer PHILIPS PW2404 and Automatic Charger PW2540 (Malvern Panalytical B, Madrid, Spain) equipped with a rhodium anode (Rh) tube with 4 kW of power, five analyzer crystals (Fli 200, Fli 220, Pe, Ge, and Px1), and three detectors: xenon sealing, scintillation, and gas flow. In the quantitative analysis, a calibration for geological samples was available, with international reference standards. The major elements determined were Al₂O₃, P₂O₅, K₂O, CaO, SiO₂, TiO₂, MnO, Fe₂O₃, MgO, and Na₂O. To analyze the major elements, beads from the samples were prepared by fusion with a Quielab pearl.

Images of the treated samples with in situ heating at 1000 °C in H₂ atmosphere were taken with the JEOL 5600 scanning electron microscope equipped with a tungsten electron gun. Images of the treated samples with ex situ abrupt heating at 1000 °C in ambient atmosphere were taken with the JEOL-6610LV scanning electron microscope at 20 kV. The samples were coated with gold.

XRD patterns of the samples, previously ground with an agate mortar, were taken with a PANalyticalX'pert Pro (Malvern Panalytical, Malvern, UK) diffractometer. The setting conditions were 40 mA and 45 kV (Cu-K α radiation; $\lambda = 1.5418 \text{ \AA}$), 2θ range of 5–70 degrees (in which the most important phases are reflected), 2θ step scans of 0.007° , and a counting time of 1 s per step. The standard reference material used was 660a NIST LaB6 with Full Width at Half Maximum (FWHM) of 0.06° for $2\theta = 21.36^\circ$. Changes in the intensity and position of the basal reflections were used to indicate changes in the structural order and hydration states.

The thermal gravimetric analyses were made between 25 and 1100 °C on the samples. The equipment was a Mettler Toledo Stare System Thermobalance (Mettler Toledo, Columbus, OH, USA) with an alumina crucible, a heating rate of 10 °C/min, and flowing oxygen at 50 mL/min. The total mass loss was determined gravimetrically by heating the samples in air at 1000 °C.

Textural parameters of the powdered samples were determined using the ASAP 2020 equipment (Iberfluid Instruments, Barcelona, Spain) under the following conditions: nitrogen adsorption at -195.8 K, with σ_m (N_2) of 0.162 nm²; unrestricted evacuation of 30.0 mm Hg; vacuum pressure of 10 μ m Hg; evacuation time of 1 h; and temperature of sample evacuation prior to N_2 adsorption measurements of 22 °C. The data were recorded with equilibration times (p/p_0 ranging from 0.001 and 1.000) between 50 and 25 s and a minimum equilibrium delay of 600 s at $p/p_0 \geq 0.995$. Specific surface area and pore size data were determined using a mathematical description of the adsorption isotherms with the software of the equipment.

3. Results

3.1. Chemical Analyses

The chemical analyses of the Ugandan sample and the Chinese samples are in Table 2. The percentage of K_2O for CHS-20 and CHGO-20 was 4.80% and 5.08% , respectively, and is greater than 0.33% , indicating that they are “commercial vermiculite”; while the Ugandan vermiculite, with 0.36% of K_2O , is a rather pure sample [30,31].

Table 2. Percentages of the oxides of the main elements in the analyzed samples.

Element Oxides	wt. %		
	U	CHS	CHGO
SiO ₂	34.96	37.88	37.20
Al ₂ O ₃	12.05	12.08	13.62
Fe ₂ O ₃	8.38	5.29	18.39
MnO	0.11	0.04	0.16
MgO	21.52	23.15	10.04
CaO	0.36	1.16	1.39
Na ₂ O	0.14	1.51	0.30
K ₂ O	0.36	4.80	5.08
TiO ₂	1.42	1.25	2.50
P ₂ O ₅	0.11	0.01	0.10
L.O.I.	20.52	11.87	11.11
TOTAL	99.92	99.05	99.88

3.2. Loss Mass and Expansion with In Situ Heating at 1000 °C in Ambient and Reduced Atmosphere

The loss mass (wt. %) of the samples treated with in situ heating at 1000 °C in ambient and reduced atmosphere is presented in Table 3. The mass loss after in situ heating at 1000 °C in ambient atmosphere in the purest vermiculite was almost twice that of vermiculites from China. In these samples, the mass loss after in situ heating at 1000 °C in reduced atmosphere was lower than the loss after in situ heating at 1000 °C in ambient atmosphere. The percentage of mass lost by samples treated with in situ heating at 1000 °C in reduced atmosphere of Ar or H_2 was similar but lower than the percentage lost when samples were treated with in situ heating at 1000 °C in reduced atmosphere of Ar and a small amount of H_2 .

In situ heating at 1000 °C in both ambient and reduced atmospheres caused the expansion of the vermiculites and a change in their color, toasted in the first case, gray in reduced atmosphere of Ar and in a reduced H_2 atmosphere is slightly darker than that of the first sample (Figures 2–4). The color and appearance of the vermiculites from Uganda and China treated with ex situ abrupt heating at 1000 °C in ambient atmosphere were similar. The appearance of the expansion with SEM observations for the vermiculites U, CHS, and CHGO treated with in situ heating at 1000 °C in H_2 atmosphere, as an example of the images obtained under reduced atmosphere, and for the same samples treated with ex situ heating at 1000 °C in ambient atmosphere can be seen in Figure 5, Figure 6, and Figure 7, respectively. The expansion occurred at right angles to the exfoliation, but as can

be seen in Figure 5a, Figure 6a, and Figure 7a, corresponding to the vermiculites heated under a reducing atmosphere, the spread apart of the sheets in the typical accordion-like structure that occurs in this heating process was smaller than in abruptly heated samples (Figure 5b, Figure 6b, and Figure 7b).

Table 3. Loss mass (wt. %) of the investigated samples after in situ heating at 1000 °C at ambient and reduced atmosphere.

Samples	Mass Loss (wt %)
U-1000	23.5
U-1000-Ar	19.5
U-1000-5H2/95Ar	20.6
U-1000-H2	18.3
CHS-1000	12.7
CHS-1000-Ar	9.4
CHS-1000-5H2/95Ar	12.3
CHS-1000-H2	10.4
CHGO-1000	11.4
CHGO-1000-Ar	10.6
CHGO-1000-5H2/95Ar	13.2
CHGO-1000-H2	10.5



Figure 2. Appearance in hand sample of the vermiculites U treated in situ at 1000 °C and (a) in ambient atmosphere, (b) in reduced atmosphere of 5%H₂ and 95%Ar, and (c) in reduced atmosphere of 100% H₂.

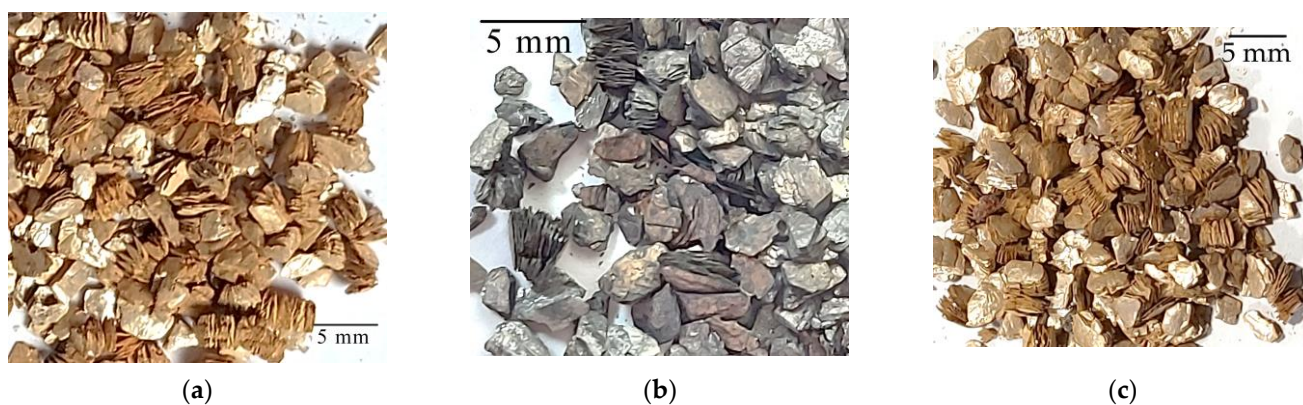


Figure 3. Appearance in hand sample of the vermiculites CHS treated in situ at 1000 °C and (a) in ambient atmosphere, (b) in reduced atmosphere of 5%H₂ and 95%Ar, and (c) in reduced atmosphere of 100% H₂.

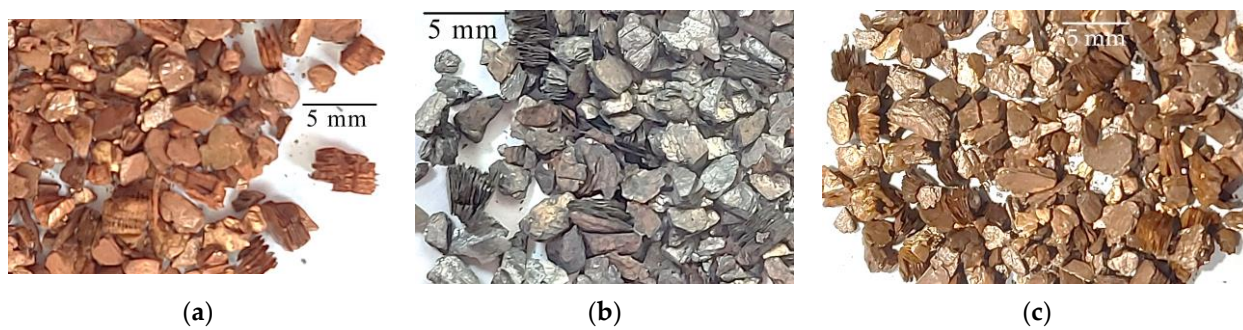


Figure 4. Appearance in hand sample of the vermiculites CHGO treated in situ at 1000 °C and (a) in ambient atmosphere, (b) in reduced atmosphere of 5%H₂ and 95%Ar, and (c) in reduced atmosphere of 100% H₂.

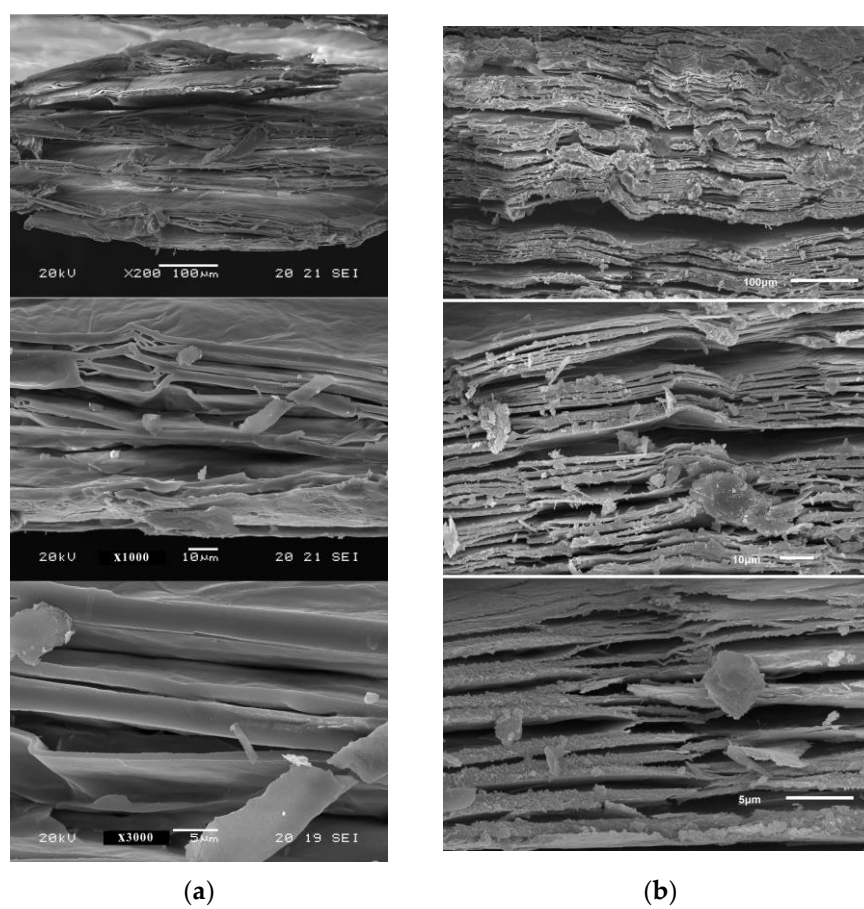


Figure 5. Appearance with SEM observations of the expansion in the vermiculites U: (a) with in situ heating at 1000 °C in H₂ atmosphere; (b) with ex situ heating at 1000 °C in ambient atmosphere.

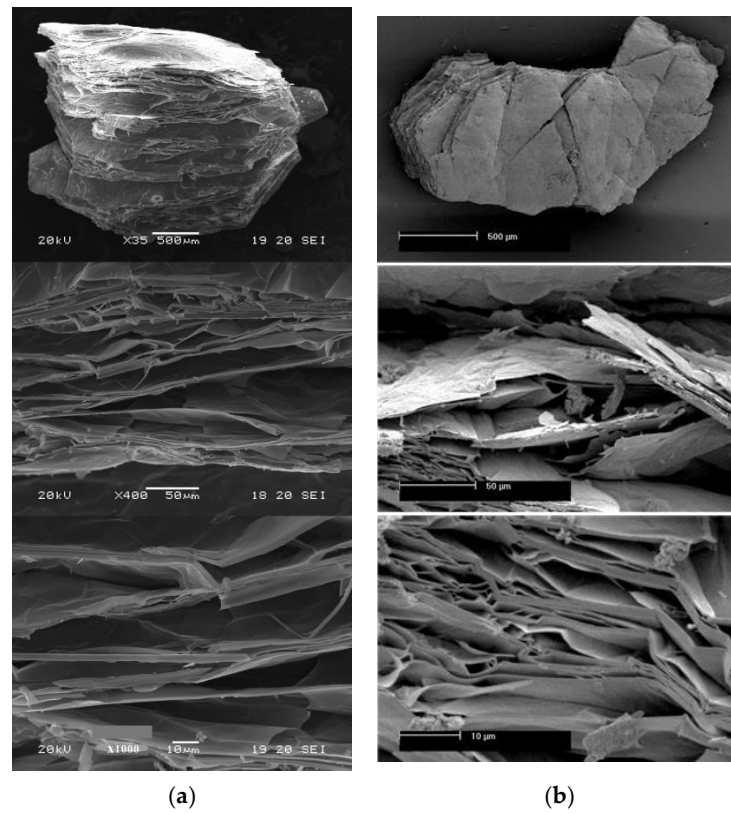


Figure 6. Appearance with SEM observations of the expansion in the vermiculites CHS: (a) with in situ heating at 1000 °C in H₂ atmosphere; (b) with ex situ heating at 1000 °C in ambient atmosphere.

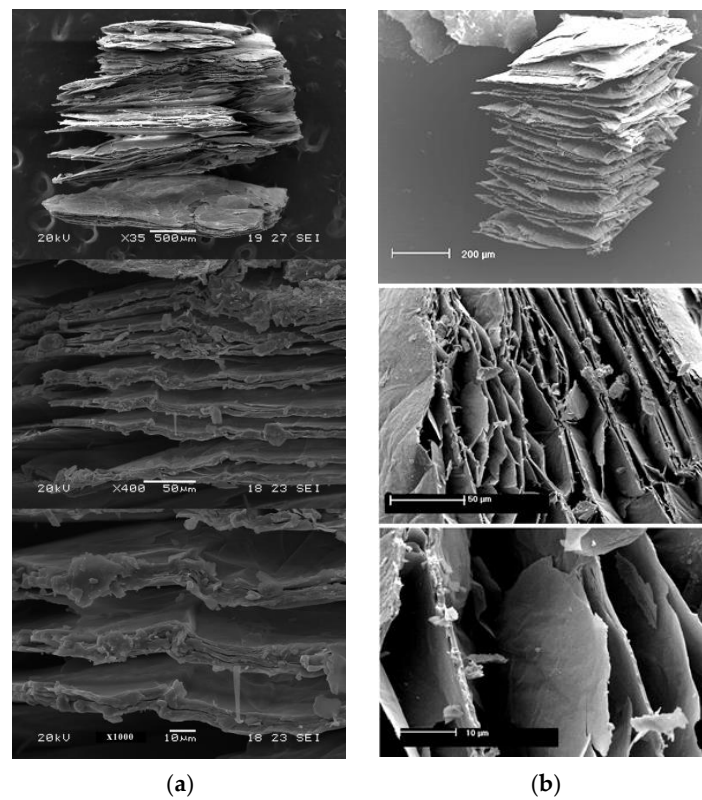


Figure 7. Appearance with SEM observations of the expansion in the vermiculites CHGO: (a) with in situ heating at 1000 °C in H₂ atmosphere; (b) with ex situ heating at 1000 °C in ambient atmosphere.

3.3. XRD Analyses

The XRD spectrum of the starting sample U (Figure 8a) consists of practically pure vermiculite (JCPDS-ICCD card 16-613). After in situ heating at 1000 °C in ambient and reduced atmosphere (Figure 8b–e), the XRD spectra of the purest vermiculite U showed a noticeable decrease in the intensity of the reflections in relation to the raw sample. In addition, vermiculite transformed to mica phlogopite (JCPDS card 16-352) and enstatite (JCPDS card 19-768) (Figure 8b), U-1000 also showed forsterite (JCPDS card 21-1257) and under Ar/H₂ atmosphere hematite (JCPDS 24-0072) appeared.

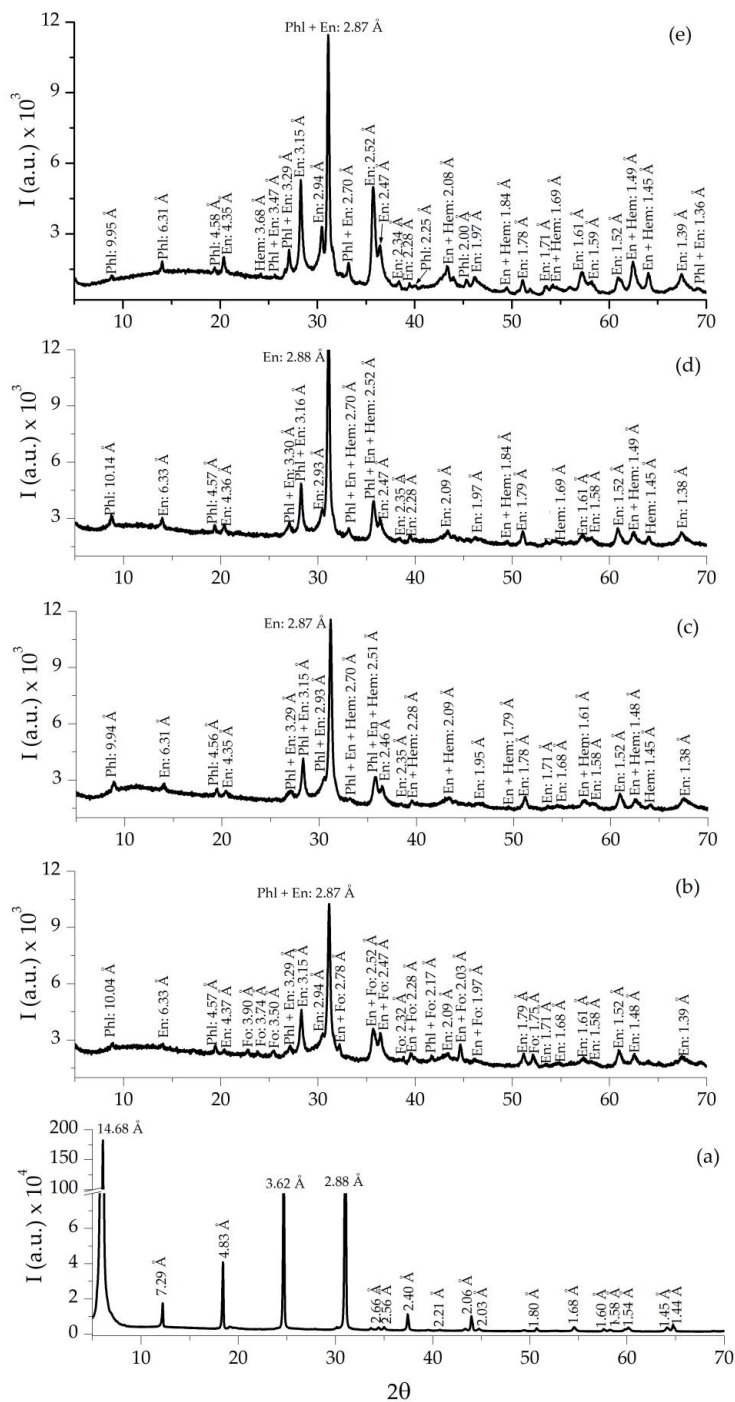


Figure 8. XRD of raw U sample (a), expanded sample under ambient atmosphere U-1000 (b), and expanded samples under reduced atmosphere U-1000-Ar (c), U-1000-5H₂/95Ar (d), and U-1000-H₂ (e). Note: Phl = phlogopite, En = enstatite, Fo = forsterite, and Hem = hematite [32].

The mineral composition of the raw sample CHS consists of vermiculite (JCPDS-ICCD card 16-613), hydrobiotite (JCPDS card 13-466) and mica biotite (JCPDS card 46-1409) (Figure 9a); after heating at 1000 °C in both air and reduced atmosphere (Figure 9b–e), the vermiculite disappeared and forsterite (JCPDS card 21-1257) appeared (Figure 9b), the reflections intensity decreased in relation to the raw sample.

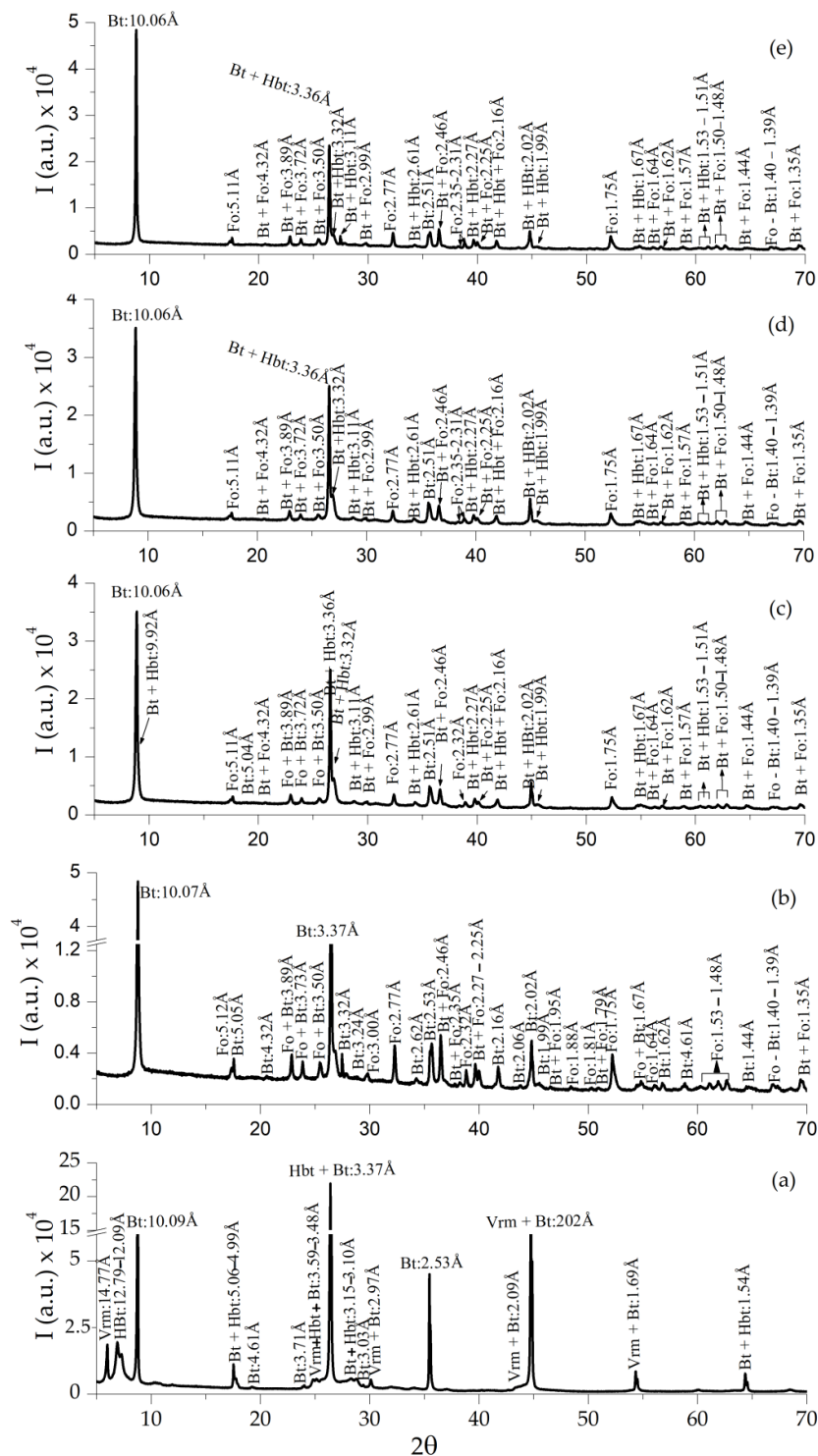


Figure 9. XRD of raw CHS sample (a), expanded sample under ambient atmosphere CHS-1000 (b), and expanded samples under reduced atmosphere CHS-1000-Ar (c), CHS-1000-5H2/95Ar (d), and CHS-1000-H2 (e). Note: Vrm = vermiculite, Bt = biotite, Hbt = hydrobiotite, and Fo = forsterite [32].

The XRD spectrum of the starting sample CHGO showed vermiculite (JCPDS-ICCD card No. 16-613), hydrobiotite (JCPDS card 13-466) and mica phlogopite (JCPDS card 16-352) (Figure 10a), after in situ heating at 1000 °C in air and reduced atmosphere (Figure 10b–e) vermiculite and hydrobiotite disappeared and enstatite (JCPDS card 19-768) forsterite (JCPDS card 21-1257) and iron crystalline phases (iron oxide–JCPDS 26-1136; hematite–JCPDS 24-0072) appeared; the reflections intensity increased in relation to the raw sample.

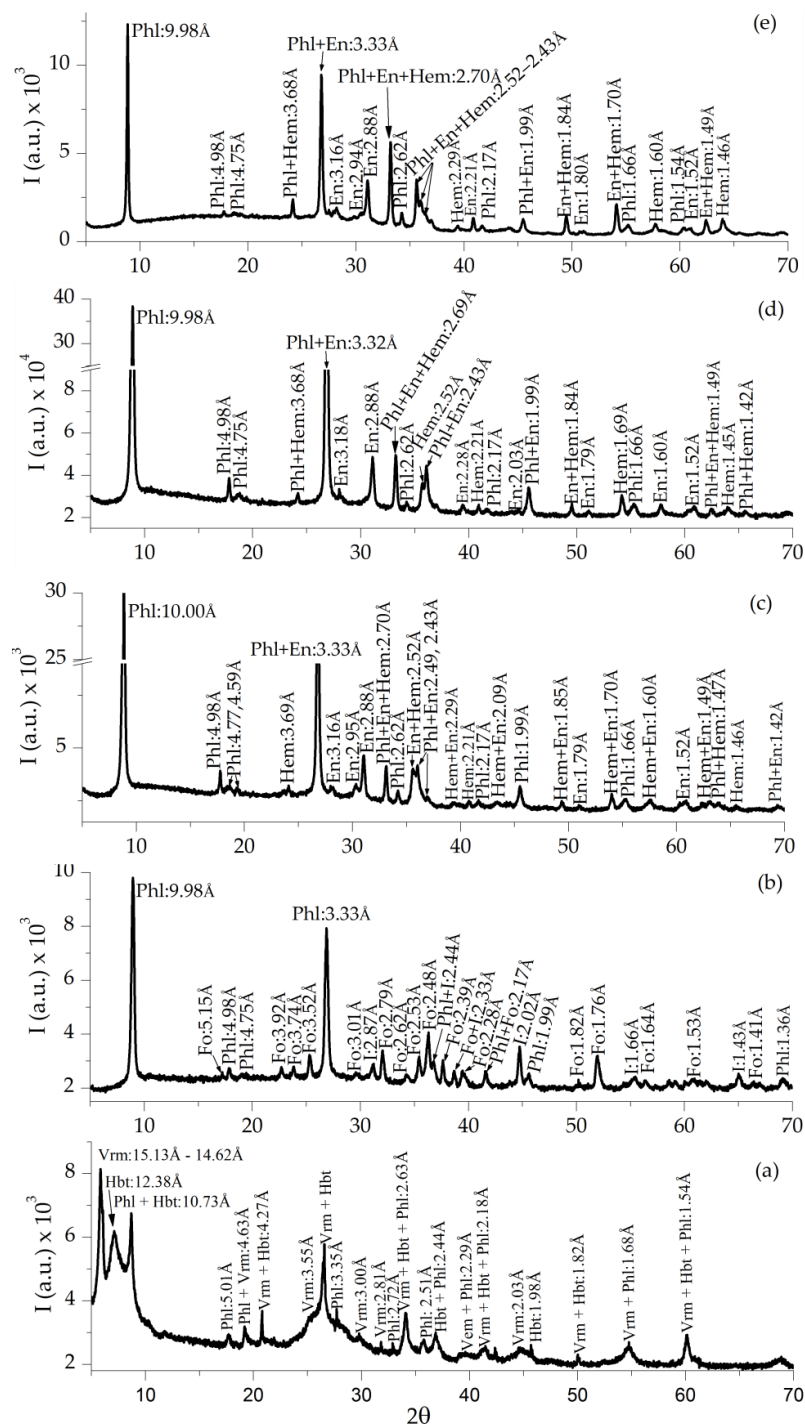


Figure 10. XRD of CHGO sample (a), expanded sample under ambient atmosphere CHGO-1000 (b), and expanded samples under reduced atmosphere CHGO-1000-Ar (c), CHGO-1000-5H2/95Ar (d), and CHGO-1000-H2 (e). Note: Vrm = vermiculite, Phl = phlogopite, Hbt = hydrobiotite, Fo = forsterite, En = enstatite, Hem = hematite, and I = iron oxide [32].

3.4. Thermogravimetric Analyses

The TG curves of the starting and heat-treated samples U, CHS, and CHGO, in both ambient and reduced atmosphere, are presented in Figure 11a, Figure 12a, and Figure 13a, respectively, from which the mass loss and/or mass gain was calculated (Table 4).

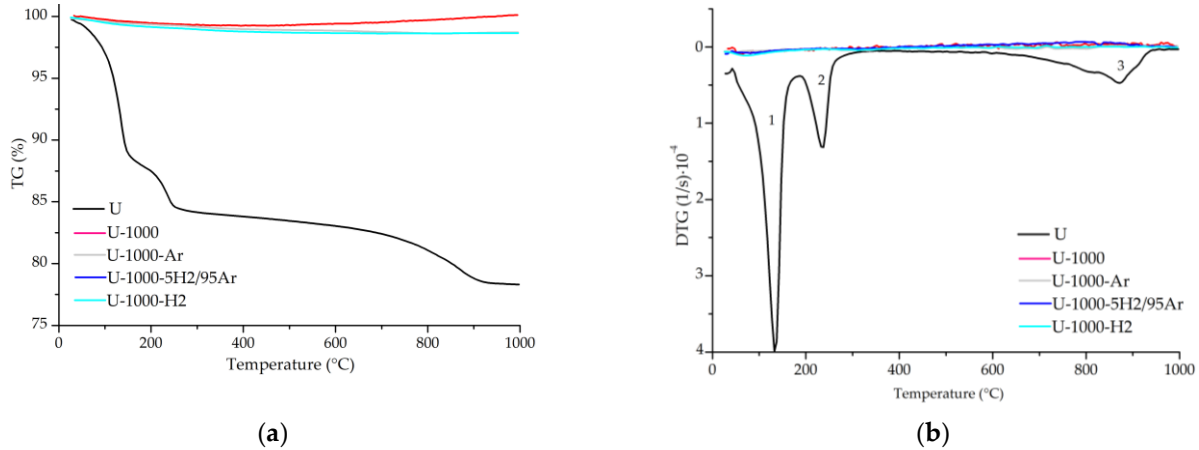


Figure 11. TG (a) and DTG (b) curves for the samples U, U-1000, U-1000-Ar, U-1000-5H2/95Ar, and U-1000-H2. Note: 1—adsorbed surface water loss; 2—interlayer water loss and interlayer cation-bound water; 3—recrystallization.

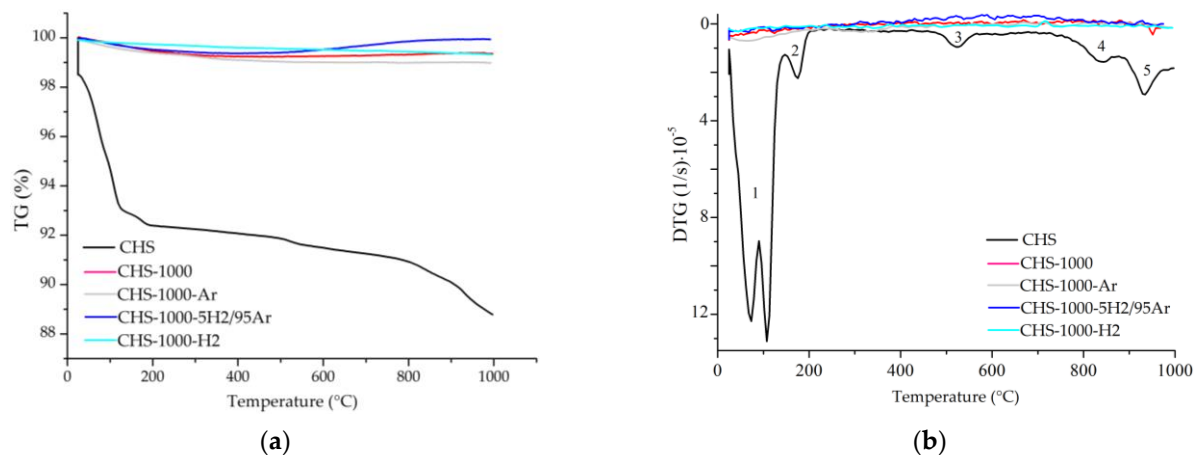


Figure 12. TG (a) and DTG (b) curves for the samples CHS, CHS-1000, CHS-1000-5H2/95Ar, CHS-1000-Ar, and CHS-1000-H2. Note: 1—adsorbed surface water loss; 2—interlayer water loss and interlayer cation-bound water; 3—loss of hydroxyls; 4—decomposition of CO₂; 5—recrystallization.

The mass loss, mainly due to water loss, in the two starting samples from China is similar and almost half that of the starting sample from Uganda. In the samples heated to 1000 °C under ambient and reduced atmosphere, there was first a slight loss of mass and then, from 800–1000 °C approximately, a slight gain of mass, except in CHGO-1000.

The DTG curves of the starting and heat-treated samples U, CHS, and CHGO, in both ambient and reduced atmosphere, are presented in Figure 11b, Figure 12b, and Figure 13b, respectively. Three different steps can be observed in the DTG curve of the raw sample U and five in the raw samples CHS and CHGO. The step ranging from approximately 50 °C to 150 °C, is due to the loss of surface adsorbed water. At temperatures above 200 °C, a loss of the interlayer water and water bound to the interlayer cations is observed. The step at temperatures between 550 °C and 650 °C is due to the loss of hydroxyls. The penultimate step in the raw samples CHS and CHGO is due to CO₂ decomposition [23,33], and the last step, at temperatures above 800 °C, is due to phase recrystallization. The response

of samples treated with in situ heating at 1000 °C in ambient and reduced atmosphere is practically linear for U and CHS samples. The appearance of the step at about 1000 °C in sample CHGO-1000-H2 could correspond to the appearance of a new crystalline phase.

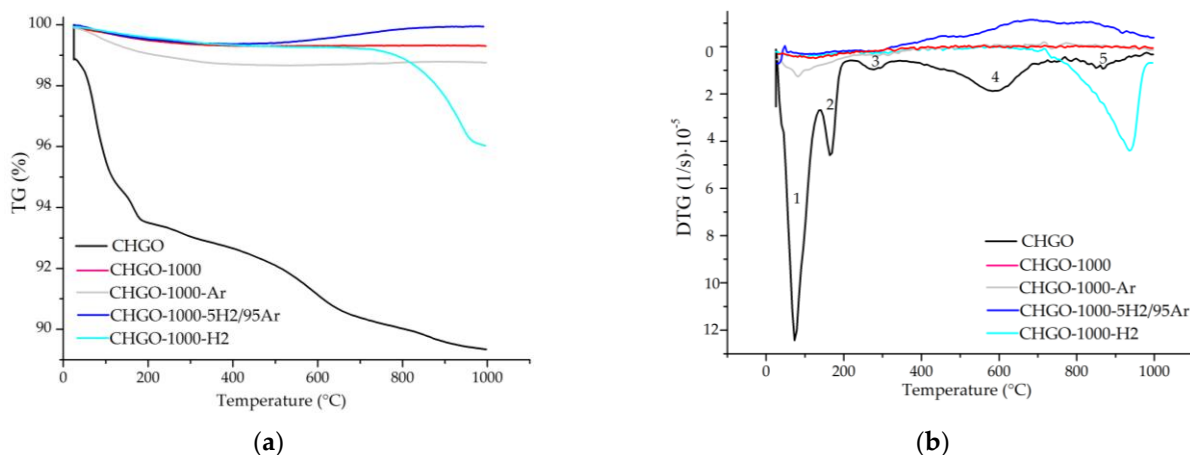


Figure 13. TG (a) and DTG (b) curves for the samples CHGO, CHGO-1000, CHGO-1000-5H2/95Ar, CHGO-1000-Ar, and CHGO-1000-H2. Note: 1—adsorbed surface water loss; 2—interlayer water loss and interlayer cation-bound water; 3—loss of hydroxyls; 4—decomposition of CO₂; 5—recrystallization.

Table 4. Loss and gain mass (%) of the investigated samples.

	Mass Loss (%)	Gain Loss (%)
U	20.00	0.00
U-1000	0.79	0.83
U-1000-Ar	0.53	0.08
U-1000-5H2/95Ar	0.83	1.08
U-1000-H2	0.92	0.01
CHS	9.02	0.00
CHS-1000	0.78	0.14
CHS-1000-Ar	0.60	0.01
CHS-1000-5H2/95Ar	0.64	0.57
CHS-1000-H2	0.22	0.12
CHGO	9.20	0.00
CHGO-1000	0.60	0.00
CHGO-1000-Ar	1.04	0.01
CHGO-1000-5H2/95Ar	0.35	2.77
CHGO-1000-H2	0.20	3.17

3.5. Textural Parameters Analyses

The nitrogen adsorption–desorption isotherms from Uganda vermiculite U and China vermiculites CHS and CHGO are shown in Figure 14a, Figure 14b, and Figure 14c, respectively. The nitrogen adsorption–desorption isotherms of the untreated and treated vermiculites from Uganda and China correspond to type IV, based on IUPAC classification, showing characteristics of mesoporous solids [34]. The slight H3 hysteresis exhibited by the raw samples is characteristic of layered particles, such as phyllosilicate group minerals, including vermiculite [18]. Hysteresis decreased with heat treatment in situ, regardless of the type of atmosphere, i.e., the adsorption–desorption isotherm gains reversibility, indicating that the materials resulting from the thermal treatment in situ lose porosity; the decrease is greater in Chinese vermiculites than in Ugandan vermiculite. The specific surface area (S_{BET}), adsorption capacity (Q_m), total pore volume (V_p), pore size (nm), BET constant (C), and correlation coefficient (R^2) values obtained from the adsorption–desorption experi-

ments are shown in Table 5. The specific surface area (S_{BET}) was measured using the BET mathematical model. The total pore volume (V_p) refers to the volume occupied by the adsorbate within the adsorbent at a given pressure (usually close to $p/p_0 = 1$). The V_p expresses the volume occupied by the pores in a unit mass of solid and is expressed as mmol/g. The model used for the pore size calculation has been the Barrett–Joyner–Halenda (BJH) model [35], which is applied only to type IV isotherms, considering the Faass correction [36], which adjusts for the change in thickness of the multilayer during the intervals in which the cores are not emptied. The C values of the investigated untreated and treated samples, ranging between 44 and 156, confirmed the validity of the BET method. The C values higher up to 150 are generally associated either with adsorption on high-energy surface sites or the filling of narrow micropores. The C values lower than 50 indicate there is an appreciable overlap of monolayer and multilayer adsorption, and the precise interpretation of nm is questionable [19]. The R^2 values above 0.999 indicate the high correlation of the data.

Table 5. Specific surface area (S_{BET}), adsorption capacity (Q_m), pore volume (V_p), BET constant (C), and correlation coefficient (R^2) of nitrogen adsorption–desorption measurements for raw and treated vermiculites.

Sample	S_{BET} (m^2/g)	Q_m ($\text{mmol}/\text{g STP}$)	V_p ($\text{mmol}/\text{g STP}$)	Pore Size (nm)	C	R^2
U	11.70 ± 0.1	0.12	0.005	2.93	55.1	0.9999
U-1000	10.63 ± 0.1	0.11	0.003	2.94	56.9	0.9995
U-1000-Ar	9.53 ± 0.1	0.10	0.002	2.90	58.4	0.9996
U-1000-5H2/95Ar	9.40 ± 0.1	0.10	0.003	2.95	69.7	0.9996
U-1000-H2	11.48 ± 0.1	0.12	0.004	2.93	80.3	0.9997
CHS	15.40 ± 0.1	0.16	0.003	2.95	137.5	0.9998
CHS-1000	5.98 ± 0.03	0.06	0.002	2.92	87.4	0.9997
CHS-1000-Ar	4.23 ± 0.02	0.04	0.001	2.92	80.4	0.9999
CHS-1000-5H2/95Ar	3.80 ± 0.03	0.04	0.001	2.52	45.2	0.9994
CHS-1000-H2	4.94 ± 0.04	0.05	0.002	3.24	231.9	0.9998
CHGO	12.10 ± 0.1	0.16	0.007	2.52	155.6	0.9996
CHGO-1000	3.59 ± 0.02	0.04	0.001	2.93	63.0	0.9997
CHGO-1000-Ar	4.54 ± 0.04	0.05	0.001	2.52	55.9	0.9994
CHGO-1000-5H2/95Ar	2.06 ± 0.02	0.02	0.001	2.95	44.0	0.9994
CHGO-1000-H2	3.60 ± 0.03	0.04	0.001	2.93	68.8	0.9995

The S_{BET} and Q_m values of the samples from Uganda and China samples treated with in situ heating at 1000 °C in ambient and reduced atmosphere are lower than those of the starting sample being these differences are greater for the Chinese vermiculites. The lowest S_{BET} and Q_m values were provided by samples treated with in situ heating at 1000 °C in a reduced atmosphere with 5% H₂ and 95% Ar. The V_p value was also reduced in samples treated with in situ heating at 1000 °C in ambient and reduced atmospheres; this reduction was greater in the CHGO samples. In relation to pore size, it seems that the thermal treatment did not affect the pore size appreciably.

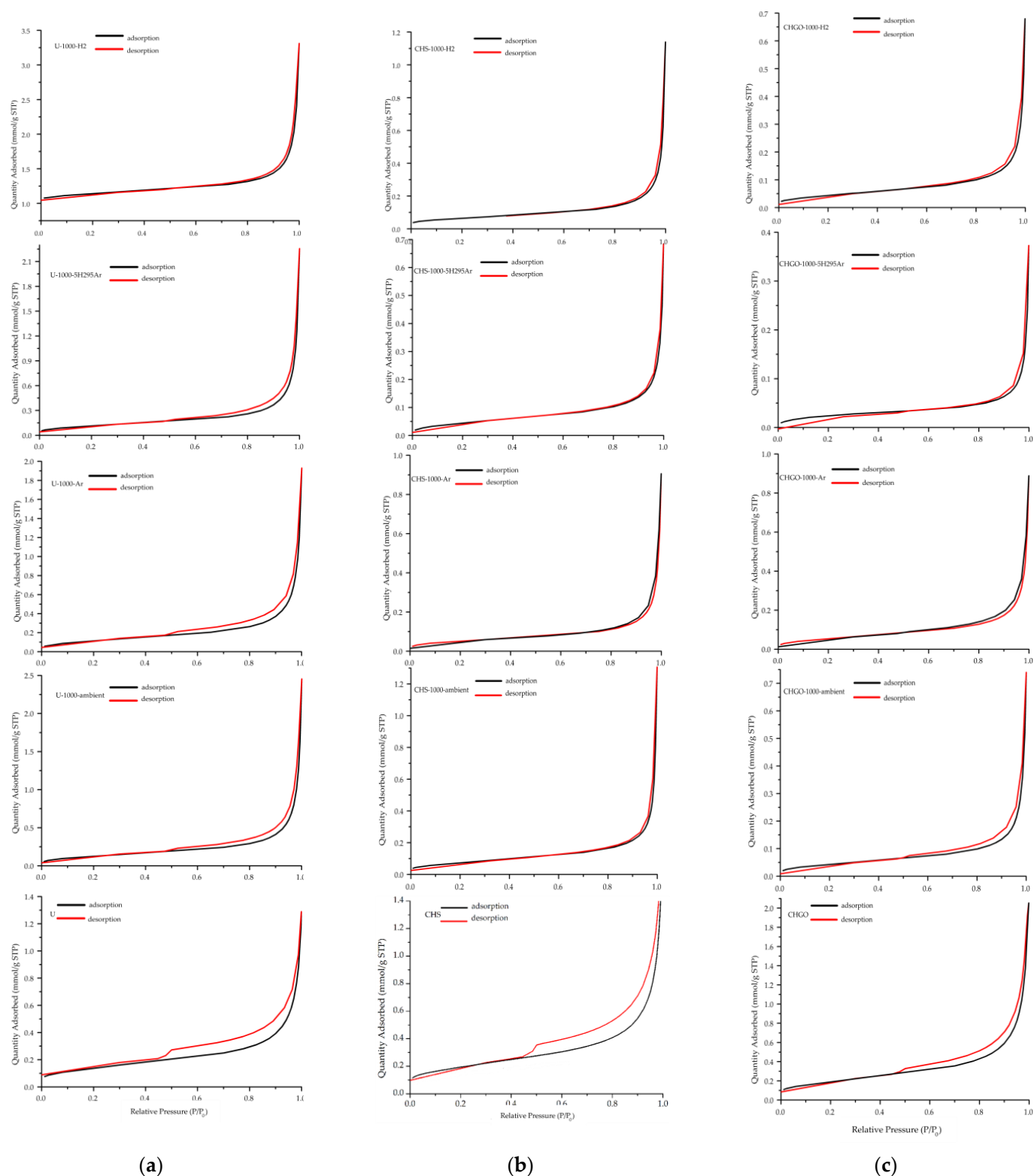


Figure 14. BET isotherms for raw samples and samples treated with in situ heating at 1000 °C in ambient and reduced atmosphere from Uganda (a) and China: CHS (b) and China: CHGO (c). Relative pressure (P/P_0).

4. Discussion

The response of vermiculites treated with in situ heating at 1000 °C in ambient and reduced atmospheres was the transformation of its surface and volumetric properties, color

appearance, and crystalline structure due to dehydration. The main differences in the physical transformation of the investigated vermiculites due to in situ heating at 1000 °C in ambient and reduced atmospheres, in relation to the ex situ abrupt heating at 1000 °C [8], are the apparent color change and the expansion that produced less separation of the exfoliation sheets. The structural transformation was greater in the purest vermiculite from Uganda and less in the most micaceous ones, corresponding to the China vermiculites. In the Ugandan vermiculite, both in ambient and reduced atmosphere, vermiculite disappeared, and phlogopite began to appear, in addition to enstatite and forsterite. With pure Ar atmosphere, forsterite disappeared, and the intensity of the reflections decreased slightly; with the mixture of Ar and a very small percentage of H₂, the phlogopite and enstatite phases were maintained, and a small amount of hematite appeared; finally, with pure H₂, heating caused a loss of phlogopite with a gain of enstatite. Similarly, in the case of the in situ heating treatment described by Marcos et al. [8], a very pure phase such as Santa Olalla vermiculite, with characteristics similar to those of Uganda, the reflection with *d*-spacing of 10 Å, due to muscovite or dehydrated vermiculite, appeared at 400 °C and was maintained until 800 °C but disappeared at 1000 °C. In the current study, the Ugandan vermiculite treated with ex situ abrupt heating at 1000 °C in ambient atmosphere showed dehydration and transformation into enstatite [8,37]. With the heating methodology used in this study, in both samples, CHS and CHGO mica (biotite and phlogopite, respectively) remained, while vermiculite disappeared and forsterite and/or enstatite appeared; in addition, iron oxides appeared in the CHGO sample as hematite, due to its higher iron content. For the CHS sample, the same transformation is maintained during heating in ambient and reduced atmospheres; the reflection intensity decreased under ambient and reduced atmosphere and hydrobiotite remained under reducing conditions. In the CHGO sample, the forsterite disappeared, and the intensity of the reflections of the new phases increased, as did the crystallinity and structural order. Correspondingly, with the in situ heating treatment described by Marcos et al. [8], in the structure of the CHS sample, small crystallites of mica coexisted with vermiculite with different hydration states at 1000 °C [8]. In the CHGO sample, above 300 °C up to 1000 °C, a micaceous phase with a *d*-spacing of 10–10.2 Å would be present (related to phlogopite presence). The ex situ abrupt heating at 1000 °C in ambient atmosphere of the samples from China caused its transformation to mica and enstatite in the case of the CHS sample and only to mica in the case of the CHGO sample [8].

Such structural transformations are a dynamic process that depends on particle composition, size and shape, relative humidity, process conditions (i.e., in situ or ex situ heating) [8], and type of atmosphere during heating (i.e., ambient or reducing).

The presence of phases, such as enstatite and forsterite, is due to the chemical composition of the vermiculite, which satisfies the compositional parameters of the SiO₂–Al₂O₃–MgO phase diagram [38].

The increase or decrease in the intensity of the reflections shown by heat-treated vermiculites appears to be related to the phases present in the starting samples and the resulting phases after treatment, i.e., it depends on the energy required for one or the other mineral transformation to occur.

The difference between the very slight mass loss shown in the thermogravimetric analyses of samples treated with in situ heating at 1000 °C in ambient and reduced atmosphere versus a much larger mass loss of such samples treated with ex situ abrupt heating at 1000 °C in ambient atmosphere (10.0% for U, 18.1% for CHS, and 6.6% for CHGO) is due exclusively to the heating conditions, regardless of the type of atmosphere. The mass gain shown in the thermogravimetric analyses of the samples treated with in situ heating at 1000 °C in ambient and reduced atmospheres could be due to adsorption by the samples of the gas used in the said analyses at high temperature, as a consequence of their textural and structural transformation due to the heat treatment conditions to which they were exposed. The analyses were run under oxygen and nitrogen atmospheres, and the results were similar. On the other hand, the different steps observed in the DTG curves, besides

water loss, are related to the different mineral transformations (i.e., loss of hydroxyls, decomposition of CO_2 , and recrystallization processes) observed in the heated samples.

The transformation of the vermiculites due to physical treatments by heating at high temperatures in ambient and reducing atmosphere is the cause of the differences in the BET results in the investigated samples. Comparing the results of the textural parameters obtained in this investigation of the vermiculites from Uganda and China treated with in situ heating at 1000 °C in ambient atmosphere with those obtained for the same samples treated with ex situ heating at 1000 °C in ambient atmosphere (Table 6), it can be stated that the S_{BET} , Q_m , and V_p values of the first samples are lower, although the pore size is generally higher. Therefore, the decrease in these values corroborates the observations of the SEM images that show how the expansion produced less separation of the sheets.

Table 6. Specific surface area (S_{BET}), adsorption capacity (Q_m), pore volume (V_p), BET constant (C), and correlation coefficient (R^2) of nitrogen adsorption–desorption measurements for vermiculites heated at 1000 °C in ambient atmosphere for 1 min.

Sample	S_{BET} (m^2/g)	Q_m ($\text{mmol}/\text{g STP}$)	V_p ($\text{mmol}/\text{g STP}$)	Pore Size (nm)	C	R^2
U-1000	13.2 ± 0.0	0.14	0.06	2.52	184.7	0.9999
CHS-1000	8.33 ± 0.1	0.09	0.006	2.51	86.2	0.9996
CHGO-1000	9.04 ± 0.1	0.09	0.006	2.64	135.1	0.9998

In summary, the specific applications of commercial heat-treated vermiculite may vary depending on the textural parameters (surface area and porosity), degree of sheet spread apart achieved, and other characteristics related to their mineral compositions at the end of the thermal process. These properties of raw vermiculites can be modulated by using different types of heat treatment (in situ and ex situ) and atmosphere (ambient and reduced), here described in the current study, in order to adapt them to the final industrial and technological purpose.

5. Conclusions

To the authors' knowledge, this is the first time that results of vermiculites treated with in situ heating at 1000 °C in a reducing atmosphere have been presented.

The response of different commercial vermiculites to in situ heating at 1000 °C in ambient and reduced atmosphere was the transformation of its surface and volumetric properties, color appearance, and crystalline structure due to dehydration and mineral alteration processes.

In situ heating at 1000 °C in the Ar and/or H_2 atmosphere produced a lower percentage of mass loss, practically related to water content, than heating in the ambient atmosphere. The very slight mass loss shown in the thermogravimetric analyses of samples treated with in situ heating at 1000 °C in the conditions presented in this study seems to be due exclusively to the heating conditions, regardless of the type of atmosphere.

The decrease in the specific surface area, adsorption capacity, and pore volume values of the samples treated with in situ heating at 1000 °C in ambient and reduced atmosphere related to those values obtained for the samples treated with ex situ abrupt heating at 1000 °C in ambient atmosphere corroborated that the expansion in the first type of thermal treatment produced less separation of the exfoliation sheets than the expansion of the samples in the second type of thermal treatment.

These textural changes, together with the structural ones, could play a fundamental role in the choice of industrial and technological applications for which these materials could be used.

Finally, it can be concluded that the properties of raw vermiculites can be modulated using different types of heat treatment (in situ and ex situ) and atmosphere (ambient

and reduced) for the purpose of adapting them to the final industrial and technological application.

Author Contributions: Conceptualization, C.M.; methodology, C.M., A.L., P.Á.-L. and F.L.; software, C.M., A.L., P.Á.-L. and F.L.; validation, C.M.; formal analysis, C.M., A.L. and P.Á.-L.; investigation, C.M., A.L., P.Á.-L. and F.L.; resources, C.M., A.L., P.Á.-L. and F.L.; data curation, C.M.; writing—original draft preparation, C.M., A.L. and P.Á.-L.; writing—review and editing, C.M.; visualization, C.M.; supervision, C.M. and P.Á.-L.; funding acquisition, P.Á.-L. and F.L. All authors have read and agreed to the published version of the manuscript.

Funding: This research was funded by the Ministry of Science and Innovation, Spain, projects PCI2019-111931-2 and PID2021-126098OB-I00/701AEI/FEDER10.13039/501100011033, and the European Regional Development Fund (ERDF)-Next Generation/EU program.

Data Availability Statement: No new data were created.

Acknowledgments: The authors would like to acknowledge the technical assistance provided at the Scientific-Technical Services, University of Oviedo, Spain, executing X-ray diffraction, fluorescence analyses, thermal gravimetric analyses, and textural parameters.

Conflicts of Interest: The authors declare no conflicts of interest.

References

- Mathieson, A.M.; Walker, G.F. Crystal structure of magnesium-vermiculite. *Am. Min.* **1954**, *39*, 231–255.
- Vali, H.; Hesse, R. Identification of vermiculite by transmission electron microscopy and x-ray diffraction. *Clay Miner.* **1992**, *27*, 185–192. [[CrossRef](#)]
- Collins, D.R.; Fitch, A.N.; Catlow, R.A. Dehydration of vermiculites and montmorillonites: A time-resolved powder neutron diffraction study. *J. Mater. Chem.* **1992**, *8*, 865–873. [[CrossRef](#)]
- Reichenbach, H.G.; Beyer, J. Dehydration and rehydration of vermiculites: IV. Arrangements of interlayer components in the 1.43 nm and 1.38 nm hydrates of Mg-vermiculite. *Clay Miner.* **1994**, *29*, 327–340.
- Reichenbach, H.G.; Beyer, J. Dehydration and rehydration of vermiculites: II. Phlogopitic Ca-vermiculite. *Clay Miner.* **1995**, *30*, 273–286. [[CrossRef](#)]
- Reichenbach, H.G.; Beyer, J. Dehydration and rehydration of vermiculites: III. Phlogopitic Sr. and Ba-vermiculite. *Clay Miner.* **1997**, *32*, 573–586. [[CrossRef](#)]
- Marcos, C.; Argüelles, A.; Ruíz-Conde, A.; Sánchez-Soto, P.J.; Blanco, J.A. Study of the dehydration process of vermiculites by applying a vacuum pressure: Formation of interstratified phases. *Mineral. Mag.* **2003**, *67*, 1253–1268. [[CrossRef](#)]
- Marcos, C.; Arango, Y.C.; Rodríguez, I. X-ray diffraction studies of the thermal behaviour of commercial vermiculites. *Appl. Clay Sci.* **2009**, *42*, 368–378. [[CrossRef](#)]
- Valášková, M.; Martynková, G.S. Vermiculite: Structural properties and examples of the use. In *Clay Minerals in Nature—Their Characterization, Modification and Application*; Valášková, M., Martynková, G.S., Eds.; IntechOpen: London, UK, 2012. [[CrossRef](#)]
- Suzuki, M.; Suzuki, I.S. Superparamagnetic behavior in a Ni vermiculite intercalation compound. *Phys. Rev. B* **2001**, *64*, 104418. [[CrossRef](#)]
- Hindman, J.R. Vermiculite. In *Industrial Minerals and Rocks: Commodities, Markets, and Uses*; Kogel, J.E., Trivedi, N.C., Krukowsky, S.T., Eds.; Society for Mining, Metallurgy, and Exploration: Englewood, CO, USA, 2006; pp. 1015–1027.
- Bergaya, F.; Theng, B.K.G.; Lagaly, G. (Eds.) Developments in Clay Science. In *Handbook of Clay Science*, 2nd ed.; Elsevier Ltd.: Amsterdam, The Netherlands, 2006; Volume 5.
- Klein, C.; Dutrow, B. *Manual of Mineral Science*, 23rd ed.; Wiley: New York, NY, USA, 2007; p. 716.
- Abollino, O.; Giacomino, A.; Malandrino, M.; Mentasti, E. Interaction of metal ions with montmorillonite and vermiculite. *Appl. Clay Sci.* **2008**, *38*, 227–236. [[CrossRef](#)]
- Zhang, K.; Xu, J.; Wang, K.Y.; Cheng, L.; Wang, J.; Liu, B. Preparation and characterization of chitosan nanocomposites with vermiculite of different modification. *Polym. Degrad. Stab.* **2009**, *94*, 2121–2127. [[CrossRef](#)]
- Marcos, C.; Argüelles, A.; Khainakov, S.A.; Rodríguez-Fernández, J.; Blanco, J.A. Spin-glass freezing in Ni-vermiculite intercalation compound. *J. Condens. Matter. Phys.* **2012**, *24*, 346001–346010. [[CrossRef](#)]
- Marcos Pascual, C.; Argüelles, A.; Leoni, M.; Blanco, J.A. Location of Ni²⁺ in nickel-intercalated vermiculites. *Appl. Clay Sci.* **2014**, *91–92*, 79–86. [[CrossRef](#)]
- Midgley, H.G.; Midgley, C.M. The mineralogy of some commercial vermiculites. *Clay Miner.* **1960**, *4*, 142–150. [[CrossRef](#)]
- Couderc, P.; Douillet, P. Les Vermiculites industrielles: Exfoliation, caractéristiques mineralogiques et chimiques. *Bull. Soc. Franc. Céram.* **1973**, *99*, 51–59.
- Hillier, S.; Marwa, E.M.M.; Rice, C.M. On the mechanism of exfoliation of “Vermiculite”. *Clay Miner.* **2013**, *48*, 563–582. [[CrossRef](#)]
- Marcos, C. Structural changes in vermiculites induced by temperature, pressure, irradiation, and chemical treatments. In *Clay Science and Technology*; Nascimento, G.M.D., Ed.; IntechOpen: London, UK, 2020. [[CrossRef](#)]

22. Zhang, Y.; Chen, M.; Li, G.; Shi, C.; Wang, B.; Ling, Z. Exfoliated vermiculite nanosheets supporting tetraethylenepentamine for CO₂ capture. *Results Mater.* **2020**, *7*, 100–102. [[CrossRef](#)]
23. Pereira, M.H.S.; dos Santos, C.G.; de Lima, G.M.; Oliveira-Bruziquesi, C.G.; de Alvarenga-Oliveira, V. Capture of CO₂ by vermiculite impregnated with CaO. *Carbon Manag.* **2022**, *13*, 117–126. [[CrossRef](#)]
24. Abidi, S.; Nait-Ali, B.; Joliff, Y.; Favotto, C. Impact of perlite, vermiculite and cement on the thermal conductivity of a plaster composite material: Experimental and numerical approaches. *Compos. B Eng.* **2015**, *68*, 392–400. [[CrossRef](#)]
25. Mo, K.H.; Lee, H.J.; Liu, M.Y.J.; Ling, T.-C. Incorporation of expanded vermiculite lightweight aggregate in cement mortar. *Constr. Build Mater.* **2018**, *179*, 302–306. [[CrossRef](#)]
26. Alsaman, A.S.; Ibrahim, E.M.M.; Ahmed, M.S.; Askalany, A.A. Composite adsorbent materials for desalination and cooling applications: A state of the art. *Int. J. Energy Res.* **2022**, *46*, 10345–10371. [[CrossRef](#)]
27. Cvejn, D.; Martausová, I.; Martaus, A.; Prech, J.; Vesely, O.; Cejka, J.; Lacny, Z.; Nedoma, J.; Martínek, R. Vermiculites catalyze unusual benzaldehyde and dioxane reactivity. *Catal. Today* **2021**, *366*, 218–226. [[CrossRef](#)]
28. Katsou, E.; Malamis, S.; Loizidou, M. Performance of a membrane bioreactor used for the treatment of wastewater contaminated with heavy metals. *Bioresour. Technol.* **2011**, *102*, 4325–4332. [[CrossRef](#)] [[PubMed](#)]
29. Ji, X.; Ge, L.; Liu, C.; Tang, Z.; Xiao, Y.; Chen, W.; Lei, Z.; Gao, W.; Blake, S.; De, D.; et al. Capturing functional two-dimensional nano sheets from sandwich-structure vermiculite for cancer theranostics. *Nat. Commun.* **2021**, *12*, 1124. [[CrossRef](#)] [[PubMed](#)]
30. Marcos, C.; Rodríguez, I. Exfoliation of vermiculites with chemical treatment using hydrogen peroxide and thermal treatment using microwaves. *Appl. Clay Sci.* **2014**, *87*, 219–227. [[CrossRef](#)]
31. Velde, B. High temperature or metamorphic vermiculites. *Contrib. Miner. Petrol.* **1978**, *66*, 319–323. [[CrossRef](#)]
32. Whitney, D.L.; Evans, B.W. Abbreviations for names of rock-forming minerals. *Am. Mineral.* **2010**, *95*, 185–187. [[CrossRef](#)]
33. Inguanzo, M.; Menéndez, J.A.; Fuente, E.; Pis, J.J. Reactivity of pyrolyzed sewage sludge in air and CO₂. *J. Anal. Appl. Pyrolysis* **2001**, *58–59*, 943–954. [[CrossRef](#)]
34. Thommes, M.; Kaneko, K.; Neimark, A.V.; Olivier, J.P.; Rodriguez-Reinoso, F.; Rouquerol, J.; Sing, K.S.W. Physisorption of gases, with special reference to the evaluation of surface area and pore size distribution (IUPAC Technical Report). *Pure Appl. Chem.* **2015**, *87*, 1051–1069. [[CrossRef](#)]
35. Barrett, E.P.; Joyner, L.G.; Halenda, P.P. The determination of pore volume and area distributions in porous substances. I. computations from nitrogen isotherms. *J. Am. Chem. Soc.* **1951**, *73*, 373–380. [[CrossRef](#)]
36. Faass, G.S. *Correlation of Gas Adsorption, Mercury Intrusion, and Electron Microscopy Pore Property Data for Porous Glasses*; Georgia Institute of Technology: Atlanta, GA, USA, 1981; p. 260.
37. Marcos, C.; Lahchich, A.; Álvarez-Lloret, P. Hydrothermally treated vermiculites: Ability to support products for CO₂ adsorption and geological implications. *Appl. Clay Sci.* **2023**, *232*, 106791. [[CrossRef](#)]
38. Stoch, L. Thermal analysis and thermochemistry of vitreous into crystalline state transition. *J. Therm. Anal. Calorim.* **2004**, *77*, 7–16. [[CrossRef](#)]

Disclaimer/Publisher’s Note: The statements, opinions and data contained in all publications are solely those of the individual author(s) and contributor(s) and not of MDPI and/or the editor(s). MDPI and/or the editor(s) disclaim responsibility for any injury to people or property resulting from any ideas, methods, instructions or products referred to in the content.